Effects of Dynamic Step-Step Repulsion and Autocatalysis on the Morphology of Etched Si(111) Surfaces

Yi-Chiau Huang,[1] Jaroslav Flidr,[2] Theresa A. Newton,[3] and Melissa A. Hines[3]
[1]*Department of Applied and Engineering Physics, Cornell University, Ithaca, New York 14853*
[2]*Department of Nuclear Science and Engineering, Cornell University, Ithaca, New York 14853*
[3]*Department of Chemistry, Cornell University, Ithaca, New York 14853*

(Received 2 February 1998)

Steady-state morphologies of NH_4F-etched Si(111) surfaces were investigated with scanning tunneling microscopy and kinetic Monte Carlo simulations. In stirred solutions, dynamic step-step repulsion, which is mediated by small etch pits, leads to the production of surfaces that are significantly smoother than the equilibrium limit as evidenced by terrace width distributions. In unstirred solutions, surfaces with a low density of steps show profound step bunching, while those with a high density of steps do not. This effect is attributed to step-step attractions mediated by spatially localized autocatalytic reactions. [S0031-9007(98)06125-0]

PACS numbers: 61.72.Cc, 61.72.Ff, 68.10.Jy, 81.65.Cf

For reasons that are not completely understood, the mechanical, chemical, and even electronic properties of nanoscale structures can be strongly influenced by their surface and interface morphologies. For example, atomic-scale roughness of the Si/SiO_2 interface in a metal-oxide-semiconductor field-effect transistor gate can reduce the mobility of electrons in the channel by a factor of 4 [1]. Observations such as these have stimulated a great deal of practical interest in the production of surfaces of controlled morphology, either through etching or deposition. Much of the basic research in this field has been directed towards near-equilibrium systems, where the rate of surface atom migration is comparable to the rate of reaction. In these cases, the surface morphology is determined in large part by thermodynamic considerations.

In principle, a much wider array of morphologies can be produced from chemical reactions that occur far from equilibrium; however, the evolution of surface morphology during etching and growth is poorly understood. In general, our view of chemical reactivity is based on local, atomic-scale considerations that have an effective range of no more than a few nanometers. Surface morphology develops over the course of many such reactions—hundreds or thousands of monolayers may need to be removed (or deposited) to reach the final, steady-state morphology. Is this morphology, with its potentially long length scales, a simple consequence of the cumulative effect of many short-scale events, or do more subtle perturbations come to dominate the final surface?

In this Letter, we report the *chemical production* of Si(111) surfaces that are *smoother* than the equilibrium limit as evidenced by a statistical analysis of scanning tunneling microscopy (STM) micrographs. These surfaces are produced entirely by room temperature reactions in a stirred, aqueous etchant. Under these conditions, diffusion of adatoms and surface atoms is negligible—the surface morphology is under kinetic control. In contrast, when the etching is performed in an unstirred solution, the morphology is dominated by well-separated step bunches. We will show that both of these morphologies are influenced by site-specific etching reactions, which lead to dynamic step-step repulsion [2]. In unstirred solutions, localized autocatalytic etching reactions lead to step-step attractions, which also influence the morphology. Autocatalysis may also explain the deep etch pits that are occasionally found on these surfaces.

The 1 Ω cm, B doped Si(111) surfaces used in these experiments were miscut in the $\langle 11\overline{2} \rangle$ direction, thermally oxidized and annealed, then chemically cleaned using RCA and buffered HF solutions. These procedures produced atomically rough, but extremely clean, Si(111) surfaces. The surface morphologies reported in this Letter were completely determined by the final processing step—etching in 40% NH_4F (*aq*, Transene) in a N_2 atmosphere. The etched surfaces were unreconstructed and H terminated [3]. After a brief rinse in ultrapure water (Millipore) to remove residual NH_4F, an In-Ga Ohmic contact was applied, and the sample was loaded into a UHV STM through a hydrocarbon-free loadlock. The surfaces remained horizontal during etching, and only the upper surface was analyzed.

The surface shown in Fig. 1(a) was miscut by 0.35° and etched for 1 hour *with stirring* to produce the steady-state etch morphology. This morphology is dominated by a *surprisingly regular* array of nearly straight, single bilayer steps that are each 3.1 Å in height. On an atomic scale, these surfaces are characterized by large defect-free regions ($\approx 10^4$ Å^2) separated by small pits. The larger pits have a pronounced triangular shape with $\langle 11\overline{2} \rangle$ oriented edges. The apparent protrusions in Fig. 1 are contaminants of unknown origin. These contaminants are randomly distributed, do not appear to influence etching, and are associated with long etch times. They are likely

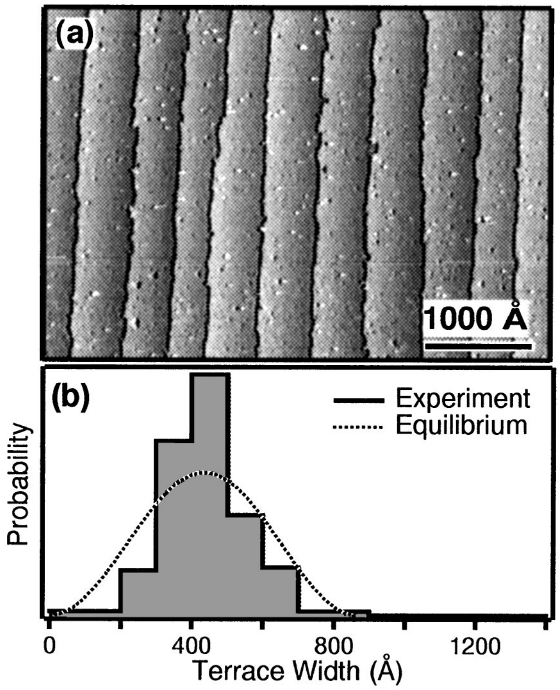

FIG. 1. Steady-state morphology of Si(111) etched in *stirred* NH$_4$F (*aq*). (a) STM images showing 3.1 Å high steps. To enhance contrast, all images combine the linear and differential topographies. (b) Distribution of terrace widths based on 168 data points. For comparison, the (calculated) equilibrium distribution is also shown.

deposited after etching, when the sample is pulled through the N$_2$-water interface.

The remarkable regularity of the etched surfaces is confirmed by the terrace width distribution shown in Fig. 1(b). For comparison, the expected distribution for a (unstrained) surface in thermal equilibrium is also shown [4]. Clearly, the distribution of steps on the etched surface is much more regular than the thermodynamic limit. Because surface curvature is determined by variations in the local step density, Fig. 1(b) shows that *etching can produce smoother surfaces than simple annealing.*

This narrow terrace width distribution is the first experimental evidence of dynamic step-step repulsion, a kinetic effect that was recently predicted by kinetic Monte Carlo (KMC) simulations of Si(111) etching [2]. Dynamic step repulsion is a form of kinetic feedback that is mediated, in this system, by the small etch pits. On this surface, etching occurs primarily at kink sites, as evidenced by the production of very straight step edges. Using KMC simulations [5], we estimate a kink/step etch rate ratio of ≈500. In this regime, the velocity of the etching step is rate limited by the nucleation of new kinks on the step edge. New kinks can be produced in two ways: direct etching of the step edge or collision of the etching step with an etch pit. The second pathway regulates the step distribution as follows. Because pits are nucleated at a constant rate by terrace etching and are destroyed by passing steps, the density of etch pits on a given terrace increases with terrace width. Therefore, both the kink nucleation rate and the velocity of the etching step are linearly proportional to the width of the preceding terrace [2]—wide terraces promote fast step etching. This proportionality results in negative feedback that favors the production of a regular array of steps.

Although other mechanisms can also produce narrow terrace width distributions, these alternatives can be ruled out. For example, dynamic step-step repulsion can also be mediated by step collisions [2]; however, this mechanism is most effective for closely spaced steps with ragged morphologies. Given the wide terraces (≈500 Å) and very straight steps in this experiment, collision-mediated step-step repulsion is of secondary importance. We can also rule out strain-mediated kinetic repulsion, as the H-terminated surface is thought to be nearly strain-free [6]. Additionally, steps oriented in the $\langle 11\bar{2} \rangle$ direction are terminated by an unstrained monohydride unit [7]. Coalescence of two $\langle 11\bar{2} \rangle$ steps leads to the production of a new (111) facet.

Surprisingly, surfaces etched in an *unstirred solution* have a dramatically different morphology. For example, Fig. 2(a) shows the steady-state morphology of a surface etched in unstirred NH$_4$F (*aq*). This morphology is dominated by *step bunching* as shown by the measured

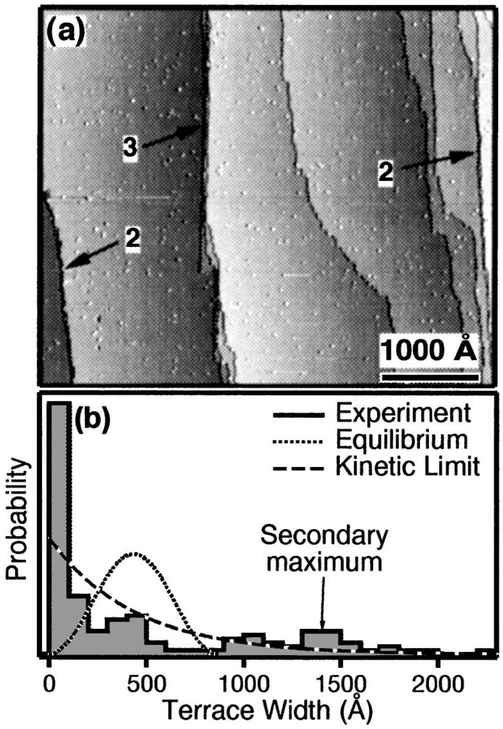

FIG. 2. Steady-state morphology of Si(111) etched in *unstirred* NH$_4$F (*aq*). (a) STM image. The number of steps in each bunch is indicated. (b) Distribution of terrace widths based on 146 data points. The equilibrium and limiting kinetic distributions are shown for comparison.

terrace width distribution [Fig. 2(b)]. Site-specific reaction kinetics *cannot* explain this distribution. The dashed line in Fig. 2(b) represents the limiting case of site-specific etching, which is reached when the rate of kink etching is infinitely faster than the rate of step etching [2]. All other site-specific kinetics produce distributions that are more Gaussian and shifted towards the mean terrace width. In comparison to this limiting behavior, the experimental distribution is strongly skewed towards narrow terrace widths and has a broad secondary maximum at high widths.

Strain-mediated step bunching can be ruled out, because bunching is also seen on surfaces miscut in the $\langle\overline{1}\overline{1}2\rangle$ direction. This surface is expected to have very different strain fields, as $\langle\overline{1}\overline{1}2\rangle$ oriented steps are terminated by a highly strained vertical dihydride group [7].

This puzzling behavior can be explained by the underlying chemical reactions. In basic fluorine solutions, etching of silicon proceeds via sequential oxidation and etching reactions

$$\equiv\mathrm{Si}\text{—}\mathrm{H} + \mathrm{OH}^- + \mathrm{H_2O} \rightarrow \equiv\mathrm{Si}\text{—}\mathrm{OH} + \mathrm{H_2} + \mathrm{OH}^-$$

$$(\equiv\mathrm{Si})_3\mathrm{Si}\text{—}\mathrm{OH} + 3\mathrm{HF} \rightarrow 3(\equiv\mathrm{Si}\text{—}\mathrm{H}) + \mathrm{SiF_3OH}\,.$$

Our macroscopic etch rate measurements show that the overall rate of silicon removal increases linearly with OH^- concentration and is independent of fluorine concentration. The first reaction, oxidation, is therefore the rate limiting step. (Back reactions are impossible. Deposition of crystalline silicon from an aqueous solution has never been observed.)

In combination, these two reactions are *autocatalytic* in OH^-. Because OH^- is both a product and a reactant in the rate limiting step, a single OH^- ion can potentially lead to the initiation of many reactions. This effect is amplified by the second reaction, which consumes HF. This reaction will also lead to a local increase in pH according to

$$\mathrm{HF} \rightleftarrows \mathrm{H}^+ + \mathrm{F}^-\,.$$

Because of this, the overall etching reaction will be *locally accelerated* in the vicinity of highly reactive regions, such as step edges. When the etchant is stirred, these concentration gradients will be reduced, and the effects of autocatalysis will be minimized.

Both of these effects can be qualitatively simulated using a simple one-dimensional model of step flow etching [8]. In the absence of autocatalysis, the etch velocity of a given step v_s is proportional to

$$v_s \propto 1 + Aw_+\,,$$

where A is a constant describing the dynamic step-step repulsion, and w_+ is the width of the terrace in front of the step [8]. Starting from an array of equally spaced steps, the resulting terrace width distribution can be calculated using KMC methods. Figure 3(a) shows the results of one such simulation. Like the experiment, this distribution is narrower than the equilibrium limit. This linear dependence on w_+ has been verified by 2D KMC simulations [2].

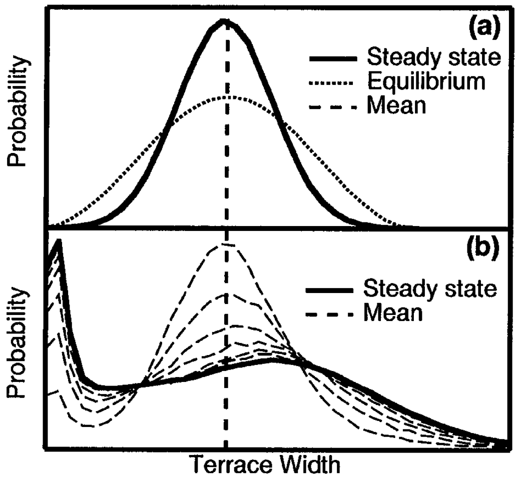

FIG. 3. Terrace width distribution from a 1D model (mean terrace width = 30 units). (a) Stirred limit showing dynamic step-step repulsion ($A = 0.017, B = 0$); (b) unstirred limit with autocatalysis included [$(A, B, f, b) = (0.017, 4, 6, 3)$]. The thin dashed lines represent the time evolution.

In the absence of stirring, the high reactivity of the step edges will lead to a local increase in the OH^- concentration at the step edges. When two steps approach one another, these regions of enhanced concentration will overlap, and both steps will accelerate. This will lead to an attractive interaction between the steps. Qualitatively, this effect can be modeled as

$$v \propto v_s[1 + B\exp(-w_+^2/f^2) + B\exp(-w_-^2/b^2)]\,.$$

In this formulation, B is a constant describing the acceleration, w_- is the width of the terrace behind the step, and f and b are constants describing the spatial extent of the OH^- buildup. The last two terms describe the interaction of the step with the OH^- associated with the preceding and succeeding steps, respectively. The asymmetry of the OH^- distribution (i.e., $f \neq b$) is attributed to the motion of the etching step.

As long as the steps are well separated (w_+, $w_- \gg f$, b), they will etch independently. If, however, a fluctuation causes two steps to approach one another, the overlap of their respective OH^- distributions will lead to an acceleration of both steps. Furthermore, if $f > b$, as expected from simple physical arguments, *the steps will bunch*. This effect can clearly be seen in Fig. 3(b). In this case, the principal maximum is due to autocatalytic step bunching. The most probable terrace width is nonzero—at this width, dynamic step-step repulsion and attractive autocatalytic effects are in balance. The secondary maximum is due to step-step repulsion between the remaining nonbunched steps. The relative magnitudes of these two maxima are determined

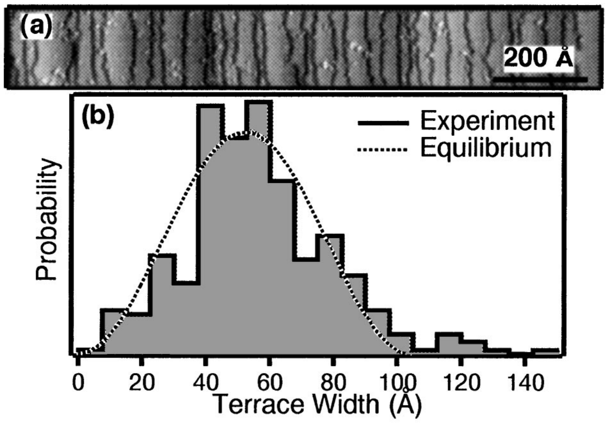

FIG. 4. Same as Fig. 2 except 3.5° miscut. (a) STM image. (b) Distribution of terrace widths based on 392 data points. The equilibrium distribution is shown for comparison.

by the variables A, B, f, and b. These simulations *qualitatively* reproduce the experimental results; however, a quantitative determination of the relevant parameters would be very difficult.

This simple one-dimensional model does make one experimentally verifiable prediction: Highly miscut surfaces should not display step bunching. When the mean terrace width is comparable to the bunching width [i.e., the principal maximum in Fig. 3(b)], there is no driving force for bunching—dynamic step-step repulsion and autocatalytic attraction are in balance.

To test this prediction, we examined the etching of surfaces with a 52 Å mean terrace width (i.e., a miscut of ≈3.5°). Figure 4(a) shows the steady-state morphology of surfaces etched in unstirred NH$_4$F (*aq*). The corresponding terrace width distribution is shown in Fig. 4(b). As predicted by our simple model, the steps on this surface showed no tendency to bunch.

Autocatalytic etching also accounts for the occasional deep etch pit that is observed after extended etching (≈1 h). For example, Fig. 5 shows a 120 Å deep pit. (The triangular shape of the etch pits is due to a 100-fold difference in the etch rates of $\langle 11\bar{2} \rangle$ and $\langle \bar{1}\bar{1}2 \rangle$ step sites [5].) The floor of the pit is relatively flat—there is no evidence of defect-nucleated etching. Since autocatalysis is a chemical manifestation of positive feedback, we tentatively attribute these etch pits to local, runaway reactions. Similar effects have been seen in macroscopic studies of autocatalytic metal etching, where localized changes in pH (up to 3.5 pH units) can be directly measured [9].

In conclusion, chemical etching can produce surfaces that are significantly smoother than the corresponding annealed surface. This chemical smoothing is due to a feedback effect, known as dynamic step-step repulsion, that is mediated by the presence of small pits on the etched terraces. Although long range in nature, this effect is solely due to site-specific chemical reactivity. In contrast, the formation of step bunches in unstirred etchants is due to the buildup of autocatalytic etch products. Because of this, transport processes in the etchant can play a major role in determining morphology.

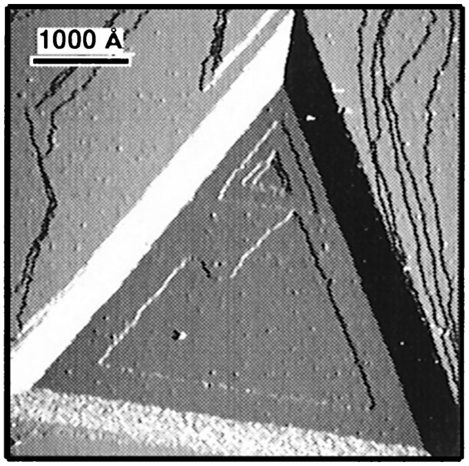

FIG. 5. 120 Å deep etch pit resulting from 1 h of etching in unstirred NH$_4$F (*aq*).

We thank Agnieszka Wesolowski, Steven M. Ewer, Lesley Hwang, and Scott Meyers for their assistance. Support of this work by the Beckman Young Investigator program is gratefully acknowledged. This work was also supported in part by the MRSEC Program of the NSF under Award No. DMR-9632275 and by the Research Corporation through the Cottrell Scholars Program. Acknowledgment is also made to the Donors of The Petroleum Research Fund for partial support of this research.

---

[1] T. Ohmi, K. Kotani, A. Teramoto, and M. Miyashita, IEEE Electron Device Lett. **12**, 652 (1991).
[2] Y.-C. Huang, J. Flidr, T. A. Newton, and M. A. Hines (to be published).
[3] G. S. Higashi, Y. J. Chabal, G. W. Trucks, and K. Raghavachari, Appl. Phys. Lett. **56**, 656 (1990).
[4] E. E. Gruber and W. W. Mullins, J. Phys. Chem. Solids **28**, 875 (1967); M. E. Fisher and D. S. Fisher, Phys. Rev. B **25**, 3192 (1982); N. C. Bartelt, T. L. Einstein, and E. D. Williams, Surf. Sci. **240**, L591 (1990).
[5] J. Flidr, Y.-C. Huang, T. A. Newton, and M. A. Hines, J. Chem. Phys. **108**, 5542 (1998).
[6] X.-P. Li and D. Vanderbilt, Phys. Rev. Lett. **69**, 2543 (1992).
[7] P. Jakob and Y. J. Chabal, J. Chem. Phys. **95**, 2897 (1991).
[8] This model was motivated by P. Bennema and G. H. Gilmer, in *Crystal Growth: An Introduction*, edited by P. Hartman (North-Holland, Amsterdam, 1973), p. 263.
[9] M. Marke and R. F. Hochman, Corrosion **26**, 5 (1970); J. C. Scully, *The Fundamentals of Corrosion* (Pergamon, Oxford, 1990), 3rd ed., Chap. 4.